

Cite this: *Chem. Commun.*, 2011, **47**, 10404–10406

www.rsc.org/chemcomm

## COMMUNICATION

## Raman active jagged-shaped gold-coated magnetic particles as a novel multimodal nanoprobe†

Morteza Mahmoudi,<sup>\*a</sup> Houshang Amiri,<sup>bcd</sup> Mohammad A. Shokrgozar,<sup>\*a</sup> Pezhman Sasanpour,<sup>f</sup> Bizhan Rashidian,<sup>fg</sup> Sophie Laurent,<sup>h</sup> Maria F. Casula<sup>i</sup> and Alessandro Lascialfari<sup>bcd</sup>

Received 9th June 2011, Accepted 26th July 2011

DOI: 10.1039/c1cc13413b

The creation of novel engineered multimodal nanoparticles (NPs) is a key focus in bionanotechnology and can lead to deep understanding of biological processes at the molecular level. Here, we present a multi-component system made of gold-coupled core-shell SPIONs, as a new nanoprobe with signal enhancement in surface Raman spectroscopy, due to its jagged-shaped gold shell coating.

The development of multifunctional engineered NPs as nanoprobes, with desired physicochemical properties, has stimulated the creation of new techniques with greater capabilities in molecular imaging and medical theranosis. Such modalities are essential for early detection and rapid treatment of diseases.<sup>1</sup> Despite extensive development of different medical imaging modalities such as X-ray, Magnetic Resonance Imaging (MRI), Positron Emission Tomography (PET), *etc.*, cellular and molecular imaging in medicine together with local therapy of pathologies still remains a dream. With the development of nanoscience this dream has the possibility to become true. The multimodal NPs have the capability, in comparison with individual NPs (*e.g.* semiconductor quantum dots, magnetic- and metallic-NPs), to be used for cellular/biomolecular tracking, to provide a high spatial resolution with high anatomical contrast together with the lack of exposure

to ionizing radiation, to follow the cells for months, and to locally deliver a drug.<sup>2,3</sup> In fact, their multimodal intrinsic characteristics allow us to use them in optical imaging, MRI, *etc.* as diagnostic probes. In addition they could be used as therapeutic agents at the molecular level, if marked with proper antibodies (by means of drug delivery, magnetic hyperthermia, *etc.*).

Among different individual NPs investigated, the super-paramagnetic iron oxide nanoparticles (SPIONs) have been recognized as one of the most important compounds, not only due to their multi-modality and multi-task ability, but also because of their excellent biocompatibility.<sup>4–7</sup> For example, SPIONs are recognized as suitable T<sub>2</sub>-weighted MRI contrast agents<sup>1</sup> even if in their standard or commercial form cannot be used for other imaging modalities. In order to make them sensible to other imaging modes (*e.g.* optical imaging), their surfaces/structures have to be modified. So the major challenge is to engineer the surface of NPs and get them functionalized, but maintaining compact sizes.<sup>8,9</sup> This could overcome some of the cited limitations and enable new imaging modes not available from each individual NP.<sup>10</sup> The combination of gold and magnetic NPs (*i.e.* gold coating on the surface of magnetic NPs) with controllable shell thickness and smooth surface can be used for multi-task applications including contrast enhancing in MRI, magnetic attraction, near-infrared (NIR) absorption, and photon scattering.<sup>11</sup> Lyon *et al.*<sup>12</sup> reported a formation of stable magnetic core-shell NPs in aqueous media through a rapid and effective route. Although several methods have been developed for the creation of direct gold coating on the surface of SPIONs,<sup>12–14</sup> the achieved direct coatings have no desired properties such as NIR responses, which are critical for *in vivo* imaging and therapy, and the compact particle size which affects tissue penetration and plasma circulation.<sup>10</sup> On the other hand, recently Jin *et al.*<sup>10</sup> reported a new generation of compact, uniform, NIR responsive gold-coated SPIONs by creating a gap between the core and the shell; in this case, a magnetically sensitive NP with strong NIR and MRI responses together with magnetomotive photo-acoustic (mmPA) imaging capability were obtained. Following a similar research line, we have prepared a new engineered generation of compact and uniform gold-coated SPIONs by creating a non-uniform gap between the core and the shell using pH stimuli-responsive polymers. This approach, not only produces a magnetically sensitive (*i.e.* detectable through MRI)

<sup>a</sup> National Cell Bank, Pasteur Institute of Iran, Tehran, Iran. E-mail: mahmoudi@biospion.com; Web: www.biospion.com; E-mail: mashokrgozar@pasteur.ac.ir; Fax: +98 2166492595; Tel: +98 2166492595

<sup>b</sup> Dipartimento di Scienze Molecolari Applicate ai Biosistemi, Università degli Studi di Milano, 20134 Milan, Italy

<sup>c</sup> CNR-Istituto di Nanoscienze, Centro S3, 41100 Modena, Italy. E-mail: Houshang.Amiri@unipv.it

<sup>d</sup> Dipartimento di Fisica "A. Volta", Università di Pavia, 27100 Pavia, Italy. E-mail: Alessandro.Lascialfari@unipv.it

<sup>e</sup> Physics Department, Islamic Azad University, Kerman Branch, Kerman, Iran

<sup>f</sup> Institute for Nanoscience and Nanotechnology, Sharif University of Technology, Tehran 14588, Iran. E-mail: pesasanpour@gmail.com; Fax: +98 2166164123; Tel: +98 2166164123

<sup>g</sup> Department of Electrical Engineering, Sharif University of Technology, Tehran 14588, Iran. E-mail: rashidia@sharif.edu

<sup>h</sup> Department of General, Organic, and Biomedical Chemistry, NMR and Molecular Imaging Laboratory, University of Mons, Avenue Maistriau, 19, B-7000 Mons, Belgium. E-mail: Sophie.Laurent@umons.ac.be

<sup>i</sup> INSTM and Dipartimento di Scienze Chimiche, Università degli studi di Cagliari, I-09042 Cagliari, Italy. E-mail: Casulaf@unica.it

† Electronic supplementary information (ESI) available. See DOI: 10.1039/c1cc13413b

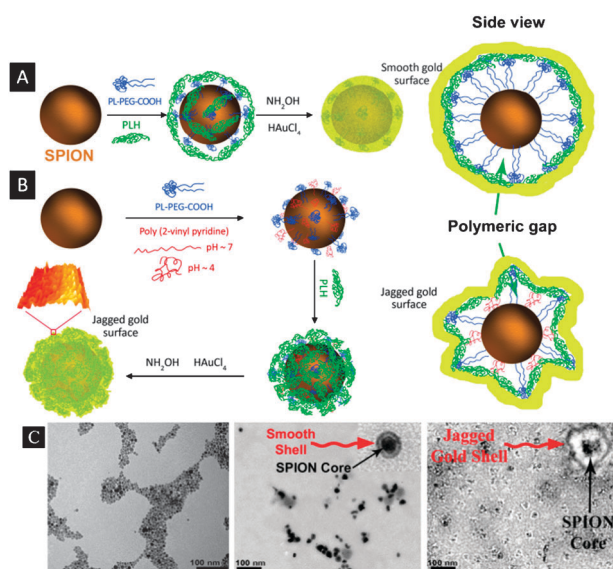


**Fig. 1** Cartoon showing the key steps involved in synthesis of (A) smooth- and (B) jagged-shaped gold-coated SPIONs with a polymeric gap, diagram is not in scale in representing the proportions of the different objects. (C) TEM images of bare SPIONs (display a formation of magnetic NPs with very narrow size distribution), smooth- and jagged-shaped gold-coated SPIONs [illustrate the existence of polymeric gap between the SPION core and gold ring together with the existence of the smooth and rough (top right panels) surface morphologies], respectively. For a better view we have presented these figures with high resolution in the ESI†.

nanoprobe with NIR and mmPA responses but it also enables the system to be used through the surface-enhanced Raman spectroscopy (SERS) which is a significant step forward for realizing imaging at the molecular level.<sup>15</sup>

Both smooth- and jagged-shaped gold shells, with a polymeric gap, were prepared at the surface of SPIONs (see Fig. 1; full experimental details are presented in ESI†). Reaction conditions were optimized in terms of polymers and gold concentrations so that the final compounds display formations of single coated SPIONs with a gold ring shell (see ESI†). Dynamic light scattering (DLS) and  $\zeta$ -potential methods were used to measure the average diameters and surface  $\zeta$ -potential of various synthesized NPs; the results, showing that the obtained NPs have very narrow size distribution, are summarized in Table S1 in ESI†. Interestingly, the  $\zeta$ -potential of the jagged-shaped gold-coated SPIONs displays two individual populations due to the significant differences between the gradient of the counter ions in keen edge of the jagged surface and smooth sections (see ESI†).

The morphology and shape of the prepared SPIONs were probed by transmission electron microscopy (TEM) and atomic force microscopy (AFM). Fig. 1C shows TEM images of bare, smooth and jagged-shaped gold-coated SPIONs. AFM images of both smooth- and jagged-shaped gold-coated SPIONs are shown in Fig. S7 in ESI†, and the insets are the corresponding magnified TEM images. The image profiles of the selected particles (see Fig. S7b and d, ESI†) in various axes show the formation of smooth- and jagged-shaped gold-coated SPIONs, respectively.

Fig. S7d (ESI†) together with its TEM image illustrates a very jagged gold ring shell on the surface of SPIONs with a polymeric gap.

Magnetic properties of bare, smooth- and jagged-shaped gold-coated SPIONs were probed *via* a SQUID magnetometer and a Nuclear Magnetic Resonance (NMR) spectrometer.

The results of zero field cooling (ZFC) and field cooling (FC) magnetization measurements are shown in Fig. S8a in ESI†. To investigate the behavior of the magnetization as a function of the applied magnetic field, hysteresis experiments in the range of  $-5T \leq H \leq +5T$  at  $T = 5$  K have been performed (Fig. S8b in ESI†). All the measurements have been corrected by the diamagnetic contributions of the sample holder. Table S2 (ESI†) presents the parameters obtained from ZFC/FC and hysteresis curves. As Fig. S8a and b (ESI†) show, magnetization in the gold-coated samples is lower than the bare NPs and it is higher in the jagged-shaped ones with respect to the smooth-shaped gold-coated samples. From Fig. S8a (ESI†) it is deduced that the blocking temperature,  $T_B$  (corresponding to the maximum in the ZFC curves), decreases from bare SPIONs towards smooth- and jagged-shaped gold-coated samples, respectively. Below  $T_B$ , the spins freeze and the system enters the blocked regime with typical out-of-equilibrium behavior.<sup>16</sup> Hysteresis loops (Fig. S8b†) display small coercive fields  $H_c$  (given in Table S2†) and a remanent magnetization  $M_r$  in both smooth- and jagged-shaped gold shell NPs rather than the bare SPIONs.

The nuclear transverse and longitudinal relaxation times have been measured at 20 and 60 MHz, at physiological temperature  $T = 37$  °C. The relaxivity measures the increase of the nuclear relaxation rates per unit of magnetic center (NPs in our case). Particularly in superparamagnetic contrast agents, the important parameter is the nuclear transverse relaxivity  $r_2$ ; in our case we obtained  $r_2 = 201.5$  (mM s)<sup>-1</sup> and  $202.2$  (mM s)<sup>-1</sup> at  $\nu = 60$  MHz for smooth- and jagged-shaped gold-coated SPIONs, respectively. The relaxivity values at 20 MHz are given in Table S2 (ESI†). Taking into account that  $r_2$  for the commercial superparamagnetic contrast agent Endorem<sup>®</sup> at 60 MHz is about  $100$  (mM s)<sup>-1</sup>, allows us to suggest our samples as MRI contrast agents. The high  $r_2$  relaxivity values of our NPs, with respect to Endorem<sup>®</sup>, cannot be justified on the basis of a susceptibility effect because the average core diameter is about 6 nm which is the same as Endorem<sup>®</sup>. On the other hand, the average hydrodynamic radius  $D_H$  of the NPs, obtained by the DLS measurements, is approximately one order of magnitude lower than Endorem<sup>®</sup> (see Table S1, ESI†). For this reason we tentatively suggest that  $r_2$  values of our samples are higher because of the reduced minimum-approach distance of the bulk water proton to the magnetic core, an event which increases the magnetic dipolar interaction.

Due to the existence of the gold shell on the surface of SPIONs, the coated SPIONs have been considered as SERS active NPs. In order to check their SERS activity, both smooth- and jagged-shaped gold-coated SPIONs were collected in a vial by a strong magnet placed on the center of the vial. The SERS activities of the collected NPs were measured *in situ*, using the confocal microprobe Raman system (see ESI†). Due to its well-documented Raman spectral data and large Raman scattering cross section,<sup>17</sup> pyridine was used as a model molecule. In order to check the capability of nanoprobe to track the pyridine interaction, 10  $\mu$ M of pyridine was added to the NPs solution and incubated for 20 min. Fig. 2 displays the SERS spectra of pyridine adsorbed on the surface of bare, smooth-, and

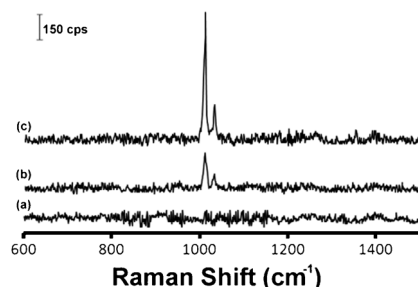


**Fig. 2** SERS spectra of pyridine absorbed on (a) bare SPIONs, (b) smooth- and (c) jagged-shaped gold-coated SPIONs.

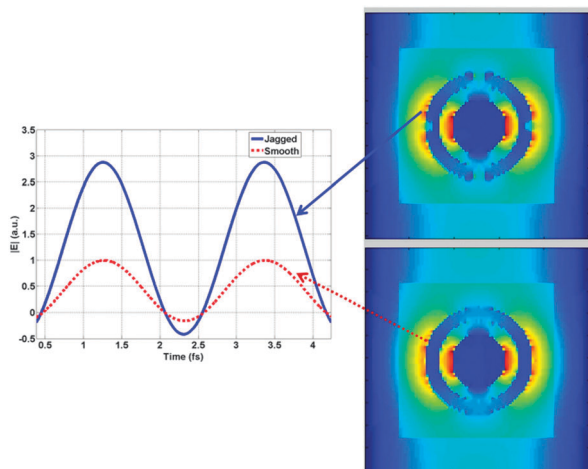


**Fig. 3** Electric field distribution around gold for the: smooth- (right-down) and jagged- (right-up) shaped gold-coated SPIONs and comparison of electric field enhancement at a point on the surface of smooth- (solid line) and jagged-shaped (dotted line) gold-coated SPIONs computed by the FDTD method.<sup>21</sup>

jagged-shaped gold coated SPIONs, respectively. According to the results, one can observe that the SERS spectra of bare SPIONs do not show any characteristic peak of pyridine. This means that the gold coated SPIONs with jagged shape display significantly higher SERS signal intensity in comparison with bare SPIONs and also with the smooth ones (see peak around  $1000\text{ cm}^{-1}$ , which corresponds to ring breathing vibration modes of pyridine adsorbed on gold surfaces).<sup>18</sup> The enhanced Raman peak intensity of the jagged gold surfaces is not only due to the higher absorbance of the pyridine on the jagged, but also due to the existence of the keen edge on the surface of jagged gold.

In order to confirm the results of SERS spectra, we have numerically analyzed the interaction of light with gold-coated SPIONs. Using the finite difference time domain (FDTD) method and exploiting the Drude model considering dispersion behavior of permittivity of gold, we have compared results of electric field enhancement according to localized surface plasmons for two cases (smooth and jagged structures). As it has been depicted in Fig. 3, enhancement of electric field in the jagged structure is about three times more than the smooth one, because of the existence of sharp edges on the gold surface. The results are in good agreement with SERS spectra shown in Fig. 2. As it has been studied before, sharp edges of gold nanostructures enhance the electric field according to the localized surface plasmon resonances.<sup>19</sup> In fact, sharp edges

have the role of local confiners of electric field lines around the structure. The difference between SERS behavior of the jagged shell and the smooth shell can be simply explained according to the lightning-rod effect (crowding of electrical fields near sharp edges) and surface plasmon resonance.<sup>20</sup>

In summary, a new class of SPION–gold core–shell NPs has been developed. In contrast to previous papers in which gold shells are deposited directly on SPIONs, the core and shell of our particles are spatially separated with a dielectric polymer layer. Using stimuli sensitive polymers, the gold shell was deposited in the jagged shape on the surface of SPIONs, with a non-uniform polymeric gap. The newly synthesized magnetic NPs show a surface enhanced Raman spectroscopy signal and MRI contrast enhancement ability, thus realizing a bimodal system. Due to their superparamagnetic properties and the metal-magnetic composition, we are also currently investigating other electronic, magnetic, optical, acoustic and thermal responses, which could allow multimodality imaging. We would finally remark that the prepared jagged gold surface will also allow simple conjugation with various types of biomolecules through thiol binding to enhance all-in-one nanoprobe properties for non-invasive molecular imaging and therapy (through e.g. drug delivery and magnetic hyperthermia) of complex diseases, thus giving a new theranostic nanosystem.

## Notes and references

- M. Mahmoudi, H. Hosseinkhani, M. Hosseinkhani, S. Boutry, A. Simchi, W. S. Journeay, K. Subramani and S. Laurent, *Chem. Rev.*, 2011, **111**, 253–280.
- M. Mahmoudi, K. Azadmanesh, M. A. Shokrgozar, W. S. Journeay and S. Laurent, *Chem. Rev.*, 2011, **111**, 3407–3432.
- H. Kobayashi, Y. Koyama, T. Barrett, Y. Hama, C. A. S. Regino, I. S. Shin, B.-S. Jang, N. Le, C. H. Paik, P. L. Choyke and Y. Urano, *ACS Nano*, 2007, **1**, 258–264.
- S. Laurent, D. Forge, M. Port, A. Roch, C. Robic, L. Vander Elst and R. N. Muller, *Chem. Rev.*, 2008, **108**, 2064–2110.
- M. Mahmoudi, M. A. Shokrgozar, A. Simchi, M. Imani, A. S. Milani, P. Stroeve, H. Vali, U. O. Hafeli and S. Bonakdar, *J. Phys. Chem. C*, 2009, **113**, 2322–2331.
- A. K. Gupta, R. R. Naregalkar, V. D. Vaidya and M. Gupta, *Nanomedicine*, 2007, **2**, 23–39.
- A. Petri-Fink and H. Hofmann, *IEEE Trans. NanoBiosci.*, 2007, **6**, 289–297.
- M. Mahmoudi, V. Serpooshan and S. Laurent, *Nanoscale*, 2011, DOI: 10.1039/c1nr10326a, in press.
- J. Cheon and J.-H. Lee, *Acc. Chem. Res.*, 2008, **41**, 1630–1640.
- Y. Jin, C. Jia, S. W. Huang, M. O'Donnell and X. Gao, *Nat. Commun.*, 2010, **1**, 1–8.
- M. Mahmoudi, S. Sant, B. Wang, S. Laurent and T. Sen, *Adv. Drug Delivery Rev.*, 2011, **63**, 24–46.
- J. L. Lyon, D. A. Fleming, M. B. Stone, P. Schiffer and M. E. Williams, *Nano Lett.*, 2004, **4**, 719–723.
- L. Y. Wang, J. W. Bai, Y. J. Li and Y. Huang, *Angew. Chem., Int. Ed.*, 2008, **47**, 2439–2442.
- Z. Xu, Y. Hou and S. Sun, *J. Am. Chem. Soc.*, 2007, **129**, 8698–8699.
- Y. C. Cao, R. Jin and C. A. Mirkin, *Science*, 2002, **297**, 1536–1540.
- S. Sun, *Adv. Mater.*, 2006, **18**, 393.
- Q. J. Huang, X. F. Lin, Z. L. Yang, J. W. Hu and Z. Q. Tian, *J. Electroanal. Chem.*, 2004, **563**, 121–131.
- D. Y. Wu, B. Ren, X. Xu, G. K. Liu and Z. L. Yang, *J. Chem. Phys.*, 2003, **119**, 1701–1709.
- P. R. Sajanlal, C. Subramaniam, P. Sasanpour, B. Rashidian and T. Pradeep, *J. Mater. Chem.*, 2010, **20**, 2108.
- P. F. Liao and A. Wokaun, *J. Chem. Phys.*, 1982, **76**, 751–752.
- A. Taflov and S. C. Hagness, *Computational Electrodynamics: The Finite Difference Time-Domain Method*, Artech House Publishers, 2005.